Görlitz – Jülich collaboration on MALA – JuDFT

February 11, 2025 │ **Johannes Wasmer**[1] Lenz Fiedler[2] Philipp Rüßmann[1] Attila Cangi[2] Stefan Blügel[1] │ [1]FZ Jülich PGI-1 [2]HZDR CASUS MLMD

Talk held at HZDR-CASUS MLMD group meeting for ongoing collaboration project via HIDA Trainee Network.

Latest version of slides are here.

My research organization

Helmholtz Association

- Largest of the four big non-university research organizations in Germany, 45k employees
- Basic & applied research
- Large facilities, accelerators, supercomputing, etc.

helmholtz.de/en

Julich Research Centre

- One of the largest in Europe, 7.5k employees
- Helmholtz Research Fields: ▶ **Information**, Energy, Earth & Environment, Matter.
- Site of first exascale computer in Europe (2025)

fzj.de/en

My funding

DAEMON   cost
EUROPEAN COOPERATION
IN SCIENCE & TECHNOLOGY

European network for data-driven materials science

WG1: Community standards: data, workflows and codes for materials design.

WG2: Representations and algorithms for materials design for "single-modality" use.

WG3: Multi-modal machine learning methods for advanced materials design.

WG4: Process-structure-property relationships in materials. Novel insights and applications.

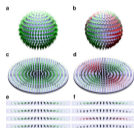**WG5:** Training, Dissemination, Exploitation, Outreach

Join via
cost-daemon.eu

My research group

Division "Quantum Theory of Materials"

Stefan Blügel

PhD advisor

Expertise DFT, Quantum magnetism, Spintronics

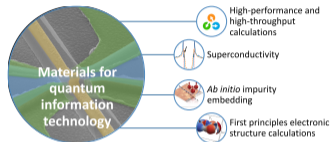## ▶ Group "Materials for Quantum Information Technology"

Philipp Rüßmann

Co-advisor

Expertise DFT, Superconductivity, Topological materials

High-performance and high-throughput calculations

Superconductivity

Ab initio impurity embedding

First principles electronic structure calculations

Code development
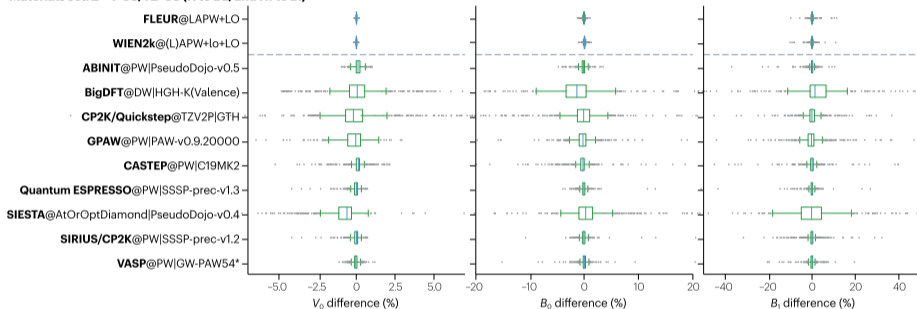
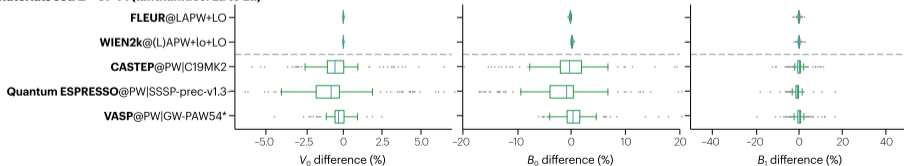fleur

spirit

JuKKR

AiiDA

judft.de // JuDFTteam

JuDFT codes accuracy

FLEUR and JuKKR are all-electron, full-potential open-source codes.

Materials set: Z = 1–56, 72–83 (H to Ba, and Hf to Bi)

FLEUR@LAPW+LO
WIEN2k@(L)APW+lo+LO
ABINIT@PW|PseudoDojo-v0.5
BigDFT@DW|HGH-K(Valence)
CP2K/Quickstep@TZV2P|GTH
GPAW@PW|PAW-v0.9.20000
CASTEP@PW|C19MK2
Quantum ESPRESSO@PW|SSSP-prec-v1.3
SIESTA@AtOrOptDiamond|PseudoDojo-v0.4
SIRIUS/CP2K@PW|SSSP-prec-v1.2
VASP@PW|GW-PAW54*

V_0 difference (%) B_0 difference (%) B_1 difference (%)

Materials set: Z = 57–71 (lanthanides: La to Lu)

FLEUR@LAPW+LO
WIEN2k@(L)APW+lo+LO
CASTEP@PW|C19MK2
Quantum ESPRESSO@PW|SSSP-prec-v1.3
VASP@PW|GW-PAW54*

V_0 difference (%) B_0 difference (%) B_1 difference (%)

[1] Bosoni et al. 2024.

AiiDA

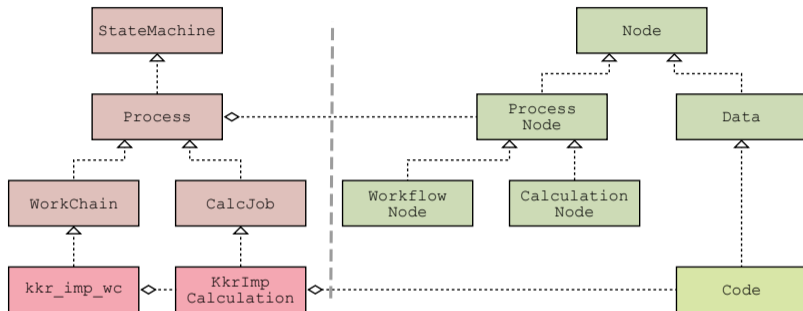**Automated Interactive Infrastructure and Database for Computational Science**

- ⚙ Workflows
- ⚓ Provenance
- ⚗ Plugin Framework
- ⭱ HPC Interface
- ⚒ Open Science
- ⊚ Open source

aiida.net

The Korringa-Kohn-Rostoker Green Function (KKR) method[1]

Green function: Definition

Time evolution operator

$$\psi(t) = e^{-iH(t-t')}\psi(t')$$

Retarded and advanced Green function

$$\psi(t) = iG^R(t-t')\psi(t') \qquad t' < t$$
$$\psi(t) = -iG^A(t-t')\psi(t') \qquad t < t'$$

$\Longleftrightarrow$

Fourier transform → energy-dependent Green function:

$$G(E) = \int_{-\infty}^{\infty} G(t)\, e^{i(E+i\varepsilon)t}\, dt = (E + i\varepsilon - H)^{-1}$$

Spectral representation via eigenfunctions-eigenvalues:

$$G(E) = \sum_i \frac{|\psi_i\rangle\langle\psi_i|}{E - \epsilon_i}$$

G(E) can be defined for complex E
(analytical continuation)

Properties of the Green function I:
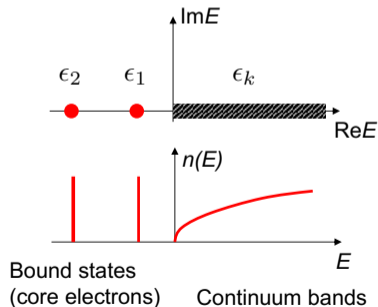## Analytical properties

Analyticity in the physical sheet $\operatorname{Im}\sqrt{E} > 0$

Poles at the eigenvalues ϵ_i and branch cut at the continuum ϵ_k

Find eigenvalues of H $\Leftrightarrow$
Locate singularities of $G(E)$

Density of states:

$$n(E) = -\frac{1}{\pi}\operatorname{Im}\operatorname{Tr}G(E)$$

Bound states
(core electrons)   Continuum bands

Properties of the Green function II:
Connection to physical properties

Definition: $(E - H)\, G(E) = 1 \implies$

Real-space representation: $(E - H)\, G(\vec{r}, \vec{r}\,'; E) = \delta(\vec{r} - \vec{r}\,')$

Expectation values of observables:

$$\langle \mathcal{O} \rangle = -\frac{1}{\pi} \mathrm{Im}\, \mathrm{Tr} \int^{E_F} dE\ \mathcal{O}\ G(E) \qquad \text{(General expression with Tr)}$$

$$= -\frac{1}{\pi} \mathrm{Im} \int^{E_F} dE \int d^3r\, d^3r'\, \mathcal{O}(\vec{r}, \vec{r}\,')\, G(\vec{r}\,', \vec{r}; E) \quad \text{(Real-space representation)}$$

Charge density: $\quad \rho(\vec{r}) = -\frac{1}{\pi} \mathrm{Im} \int^{E_F} dE\ G(\vec{r}, \vec{r}; E)$

Properties of the Green function III:
Dyson equation

Reference system Hamiltonian → New system Hamiltonian

$$H_0 \longrightarrow H = H_0 + \Delta V$$

$$G_0(E) = (E - H_0)^{-1} \longrightarrow \boxed{\begin{aligned} G(E) &= (E - H_0 - \Delta V)^{-1} \\ &= [1 - G_0(E)\,\Delta V]^{-1}\, G_0(E) \end{aligned}}$$

Dyson equation

Example: Free electrons → Electrons in a crystal

$$H_0 = -\nabla^2 \qquad H_{\mathrm{cryst}} = H_0 + V_{\mathrm{cryst}}(\vec{r})$$

Electrons in a crystal → Electrons in a crystal + impurity

$$H_0 = H_{\mathrm{cryst}} \qquad H = H_{\mathrm{cryst}} + \Delta V_{\mathrm{imp}}$$

Concept of KKR

Tessellation of space in atomic cells

Local scattering solution of Schrödinger's equation in each cell (spherical wave representation)

Multiple scattering of waves among atoms
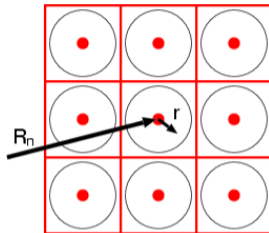→ Coupling of local solutions


Starting point:
Free electron wave function

$$\psi_{\vec{k}}(\vec{r}) = e^{i\vec{k}\cdot\vec{r}} = 4\pi \sum_L i^l \, j_l(kr) \, Y_L(\hat{k}) \, Y_L(\hat{r}) \qquad\qquad L \equiv (l, m)$$

Free electron Green function

$$g(\vec{r}, \vec{r}'; E) = -\frac{1}{4\pi} \frac{e^{ik|\vec{r}-\vec{r}'|}}{|\vec{r}-\vec{r}'|} = -i\sqrt{E} \sum_L j_l(r_<; E) \, h_l(r_>; E) \, Y_L(\vec{r}) \, Y_L(\vec{r}')$$
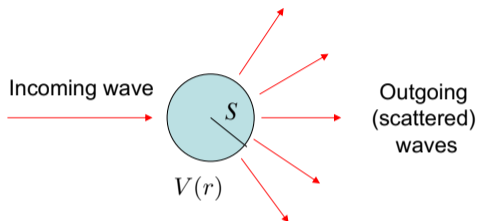
Scattering from a single potential

Incoming wave

S

Outgoing (scattered) waves

$V(r)$

Green function:

$$G(\vec{r}, \vec{r}'; E) = -i\sqrt{E} \sum_L R_l(r_<; E) \; H_l(r_>; E) \, Y_L(\vec{r}) \, Y_L(\vec{r}')$$

Regular solution $\sim r^l$

Irregular solution $\sim 1/r^{l+1}$

$L := (l, m)$

Bessel function

Hankel function

Free-space Green function:

$$g(\vec{r}, \vec{r}'; E) = -i\sqrt{E} \sum_L j_l(r_<; E) \; h_l(r_>; E) \, Y_L(\vec{r}) \, Y_L(\vec{r}')$$

Scattering from a single potential
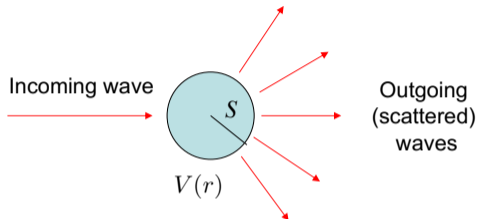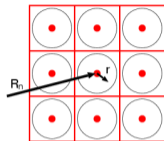

Green function:
$$G(\vec{r}, \vec{r}'; E) = -i\sqrt{E} \sum_L \underbrace{R_l(r_<; E)}_{\text{Regular solution}} \underbrace{H_l(r_>; E)}_{\text{Irregular solution}} Y_L(\vec{r}) Y_L(\vec{r}')$$

$$t_l(E) = \int_{\text{cell}} d^3r \, \underbrace{j_l(\sqrt{E}r)}_{} \, V(r) \, R_l(r; E) \qquad L := (l, m)$$

Free-space Green function:
$$g(\vec{r}, \vec{r}'; E) = -i\sqrt{E} \sum_L \underbrace{j_l(r_<; E)}_{\text{Bessel function}} \underbrace{h_l(r_>; E)}_{\text{Hankel function}} Y_L(\vec{r}) Y_L(\vec{r}')$$

KKR representation of GF

Crystal electron Green function:

$$\left(-\nabla^2 + V^n(\vec{r}) - E\right) G(\vec{r} + \vec{R}^n, \vec{r}' + \vec{R}^{n'}; E) = -\delta_{nn'}\delta(\vec{r} - \vec{r}')$$

Expanded as:

Structural Green functions

$$G(\vec{r} + \vec{R}^n, \vec{r}' + \vec{R}^{n'}; E) =$$
$$-i\sqrt{E}\sum_L R_L^n(\vec{r}_<; E) H_L^n(\vec{r}_>; E)\,\delta_{nn'} + \sum_{LL'} R_L^n(\vec{r}; E)\, G_{LL'}^{nn'}(E)\, R_{L'}^{n'}(\vec{r}'; E)$$

``*Single-site*''                          ``*Back-scattering*''
(atom in constant potential)   (contribution of all other atoms)

Free electrons:

$$g = -i\sqrt{E}\sum_L j_L^n(\vec{r}_<; E)\, h_L^n(\vec{r}_>; E)\,\delta_{nn'} + \sum_{LL'} j_L^n(\vec{r}; E)\, g_{LL'}^{nn'}(E)\, j_{L'}^{n'}(\vec{r}'; E)$$
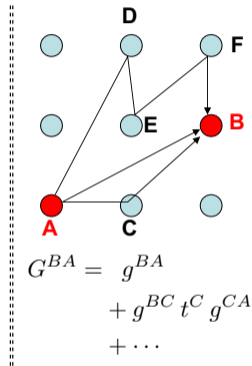
Algebraic Dyson equation

Dyson eq.: Green functions

$$G(E) = g(E) + g(E)\, V_{\mathrm{cryst}}\, G(E)$$

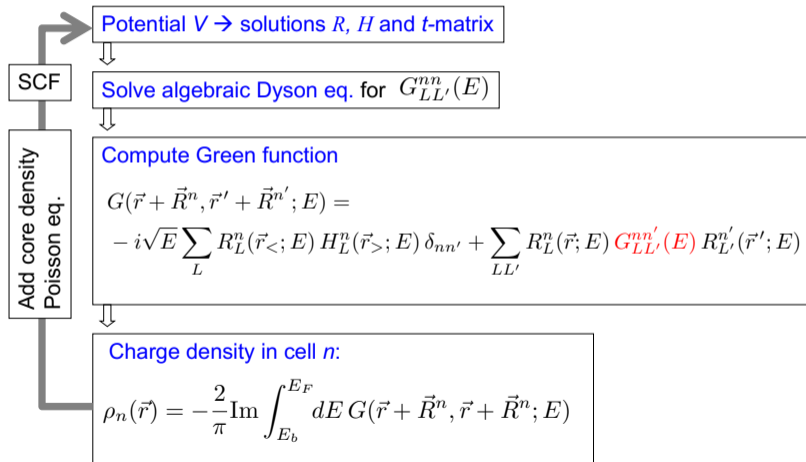Algebraic Dyson eq.: structural Green functions

$$G_{LL'}^{nn'}(E) = g_{LL'}^{nn'}(E) + \sum_{n'',L''} g_{LL''}^{nn''}(E)\, t_{l''}^{n''}(E)\, G_{L''L'}^{n''n'}(E)$$

$$
\begin{aligned}
G^{BA} = {}& g^{BA} \\
& + g^{BC}\, t^{C}\, g^{CA} \\
& + \cdots
\end{aligned}
$$

Interpretation: propagation over all scattering paths

$$G_{LL'}^{nn'} = g_{LL'}^{nn'} + \sum_{n'',L''} g_{LL''}^{nn''}\, t_{l''}^{n''}\, g_{L''L'}^{n''n'} + \sum_{n'',L''} \sum_{n''',L'''} g_{LL''}^{nn''}\, t_{l''}^{n''}\, g_{L''L'''}^{n''n'''}\, t_{l'''}^{n'''}\, g_{L'''L'}^{n'''n'} + \cdots$$

Summary of algorithm for valence-electron charge density

Potential V → solutions R, H and t-matrix

SCF

Solve algebraic Dyson eq. for $G_{LL'}^{nn}(E)$

Add core density
Poisson eq.

Compute Green function

$$G(\vec{r} + \vec{R}^n, \vec{r}' + \vec{R}^{n'}; E) =$$
$$- i\sqrt{E} \sum_L R_L^n(\vec{r}_<; E)\, H_L^n(\vec{r}_>; E)\, \delta_{nn'} + \sum_{LL'} R_L^n(\vec{r}; E)\, G_{LL'}^{nn'}(E)\, R_{L'}^{n'}(\vec{r}'; E)$$

Charge density in cell n:

$$\rho_n(\vec{r}) = -\frac{2}{\pi} \mathrm{Im} \int_{E_b}^{E_F} dE\, G(\vec{r} + \vec{R}^n, \vec{r} + \vec{R}^n; E)$$

Impurity atoms in crystals

Dyson eq.: Reference system $\rightarrow$ New system

$$G(E) = (E - H_0 - \Delta V)^{-1}$$
$$= [1 - G_0(E)\,\Delta V]^{-1}\,G_0(E)$$

Crystal   Impurity in crystal

No periodic supercell needed
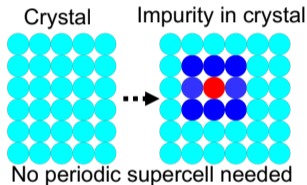
Computational effort depends on the number of *perturbed atomic potentials N* : $O(N^3)$

$$G = G_0 + G_0\,\Delta V\,G$$
$$= G_0 + G_0\,\Delta V\,G_0 + G_0\,\Delta V\,G_0\,\Delta V\,G_0 + G_0\,\Delta V\,G_0\,\Delta V\,G_0\,\Delta V\,G_0 + \cdots$$
$$= G_0 + G_0\,[\,\Delta V + \Delta V\,G\,\Delta V\,]\,G_0$$
$$:= G_0 + G_0\,T\,G_0 \qquad\qquad T \text{ is confined in the perturbed region}$$

Impurity atoms in crystals

Green function and Dyson equation for the impurity system

$$
G(\vec{r} + \vec{R}^n, \vec{r}' + \vec{R}^{n'}; E) =
$$
$$
- i\sqrt{E} \sum_L R_L^n(\vec{r}_<; E) \, H_L^n(\vec{r}_>; E) \, \delta_{nn'} + \sum_{LL'} R_L^n(\vec{r}; E) \, G_{LL'}^{nn'}(E) \, R_{L'}^{n'}(\vec{r}'; E)
$$

Summation only for the sites where t-matrix differs (impurities & surrounding atoms)

$$
G_{LL'}^{nn'}(E) = G_{0;LL'}^{nn'}(E) + \sum_{n'',L''} G_{0;LL''}^{nn''}(E) \, [t_{l''}^{n''}(E) - t_{0;l''}^{n''}(E)] \, G_{L''L'}^{n''n'}(E)
$$

Size of linear system to solve: $\texttt{DIMENSION} = N_{\mathrm{at}} \times (2l + 1)^2$

$$
G_{LL'}^{nn'}(E) = \left[[\mathbf{1} - \mathbf{G}_0(\mathbf{t} - \mathbf{t}_0)]^{-1} \mathbf{G}_0 \right]_{LL'}^{nn'}
$$

Application: Density oscillations
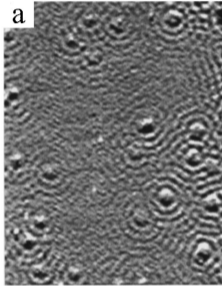
Exp.: Cu (111) surface
Petersen et al., PRB **57**,
R6858 (1998)
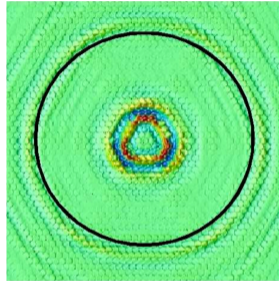
KKR calculation (Co in Cu surface)
Samir Lounis, PhD thesis (RWTH Aachen)

Other applications

Conductance in a junction:
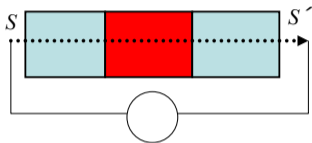
$$J = \Gamma \, \Delta U$$

$$\Gamma = -\frac{e^2 \hbar^3}{8\pi m^2} \int_S dS \int_{S'} dS' \, G(\mathbf{r}, \mathbf{r}\,'; E_F) \overleftrightarrow{\nabla}_z \overleftrightarrow{\nabla}'_z G^*(\mathbf{r}, \mathbf{r}\,'; E_F)$$

Exchange constants in ferromagnets

Heisenberg model: $\quad E = -\displaystyle\sum_{i,j} J_{ij} \, \hat{e}_i \cdot \hat{e}_j$

$$J_{ij} = -\frac{1}{4\pi} \mathrm{Im} \int^{E_F} dE \, \mathrm{Tr}_L \Delta t^i_{(\uparrow - \downarrow)} G^{ij}_{\uparrow}(E_F) \Delta t^j_{(\uparrow - \downarrow)} G^{ji}_{\downarrow}(E_F)$$
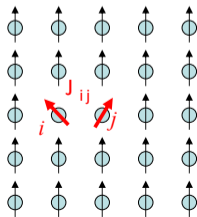
Vision: Electronic structure learning
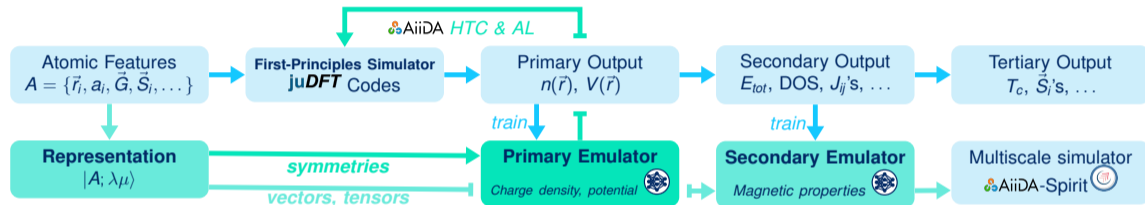
as integrated, high-level multiscale workflows

Better "initial guess"
for fast SCF convergence

Magnetic property prediction
(ML-Exc) for spin dynamics

Project "Better initial guess"
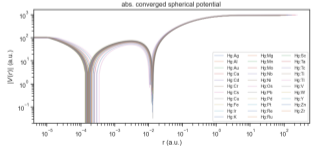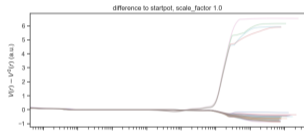
AiiDA-KKR workflows

[a] Rüßmann, Bertoldo, and Blügel 2021.

Project "Better initial guess"

Data generation

Data 10'000 impurity embeddings into elemental crystals
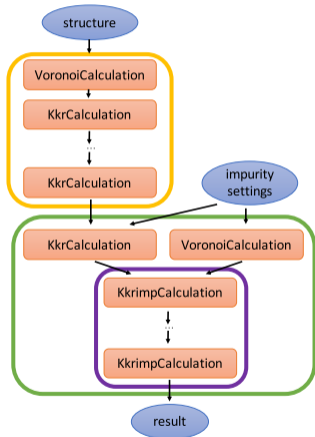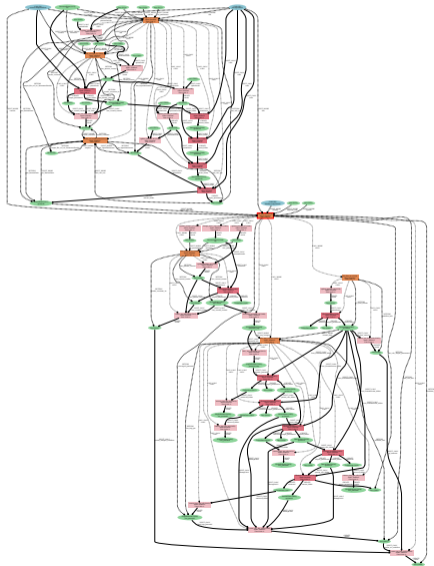
Target Electron potential difference $\Delta V_{imp}(\vec{r})$

$$\text{Green function } \mathcal{G}(E) = (E - \mathcal{H})^{-1}$$
$$\text{Perturbed system } \mathcal{H} = \mathcal{H}^0 + \Delta V$$

$$\mathcal{G} = \mathcal{G}^0 + \mathcal{G}^0 \, \Delta V \, \mathcal{G}$$

not converged

Dataset map. Rows: Element of host crystal, columns: impurity atom, color: num. calculations.
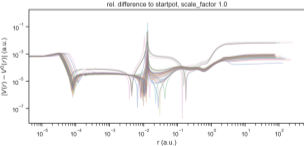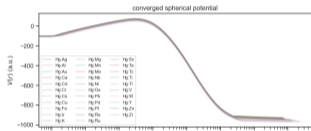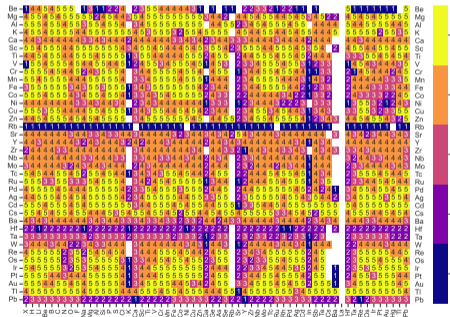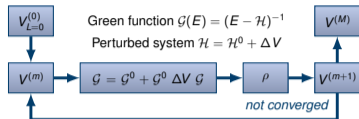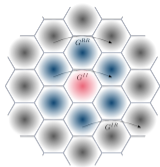
Spherical impurity potentials in first Voronoi cell of Hg:X embeddings, left upper to bottom right: V, $V - V^0$, $|V|$, $|V - V^0|$.
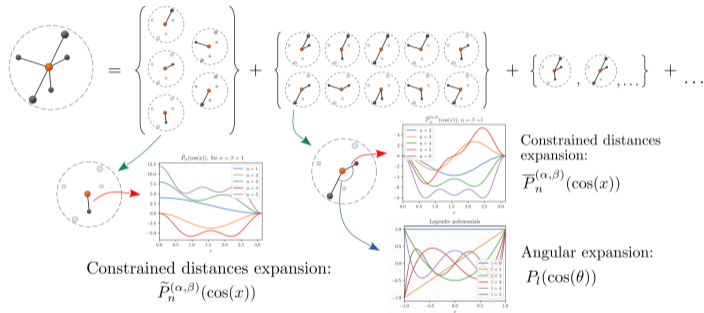
The Jacobi-Legendre framework[1]
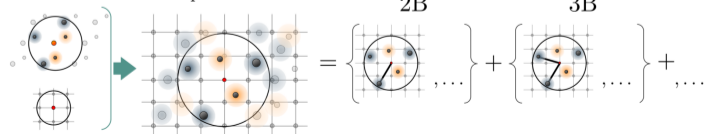
for electronic structure representation

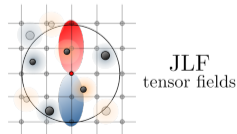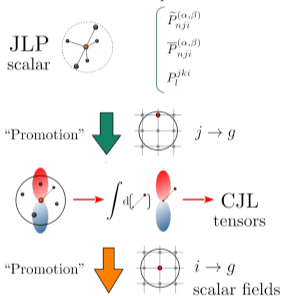[1]Michelangelo Domina 2024.

Atom-based JLCDM

- The full KKR potential is expanded in real-space Voronoi (Wigner-Seitz) cells around each atom and convoluted with shape functions

$$V(\vec{r}) = \sum_L V_L(r) Y_L(\vec{r}) \quad \text{with} \quad V_{LL'}(r) = \sum_{L''} C_{LL'L''} V_{L''}(r)$$

$$V^n(\vec{r}) = V(\vec{r} + \vec{R}^n)\Theta(\vec{r}) \quad \text{with} \quad \Theta(\vec{r}) = \sum_L \Theta_L^n(r) Y_L(\vec{r})$$
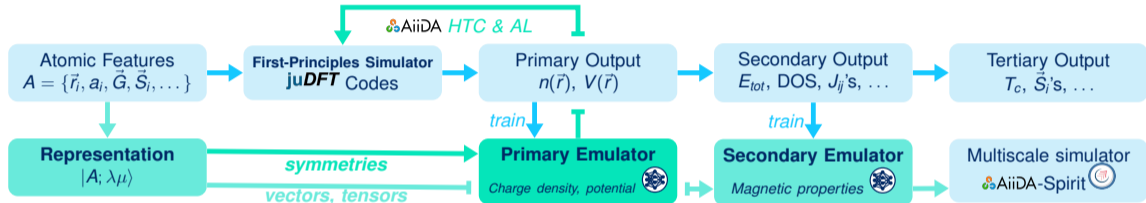
- Idea: Expand the Jacobi-Legendre grid description at each atom, instead of each grid point.

$$V(\vec{r}) = \sum_i \sum_n a_n \tilde{P}_n^{ig} + \sum_{ij} \sum_{n_1, n2, L} a_{n_1, n_2, i} \bar{P}_{n_1}^{ig} \bar{P}_{n_2}^{ij} P_L^{ijg}$$

Angular expansion $\quad \int P_L(\hat{r}_{gi} \cdot \hat{r}_{gj}) Y(\hat{r}_{gi}) \, d\hat{r} \longrightarrow \int P_L(\hat{r}_{ij} \cdot \hat{r}_{ig}) Y(\hat{r}_{ig}) \, d\hat{r}$

Vision: Electronic structure learning
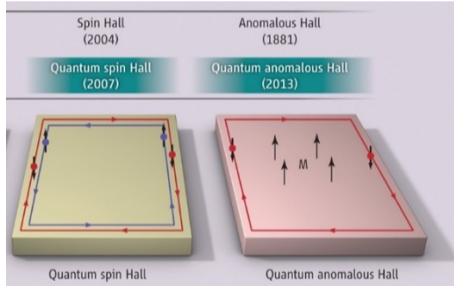## as integrated, high-level multiscale workflows

Better "initial guess"
for fast SCF convergence

Magnetic property prediction
(ML-Exc) for spin dynamics

Topological insulators and magnetic impurities

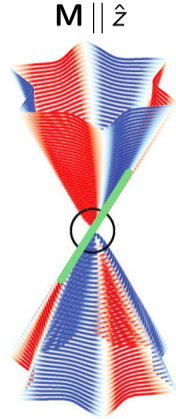
o Magnetic doping of topological insulators (**TIs**) can induce a topological phase transition

- Ferromagnetic ordering
- Out-of-plane anisotropy

Spin Hall (2004)

Anomalous Hall (1881)

Quantum spin Hall (2007)

Quantum anomalous Hall (2013)

Quantum spin Hall

Quantum anomalous Hall

S. Oh, Science **340**, 153 (2013)

(QSHE)
→ Topological insulator
Two counter propagating edge states

(**QAHE**)
One single edge state

$\mathbf{M} \parallel \hat{z}$
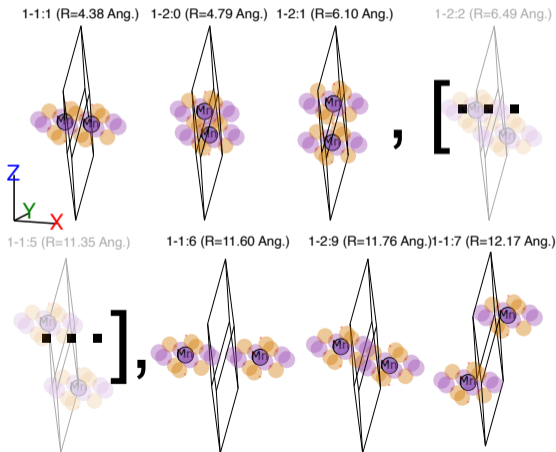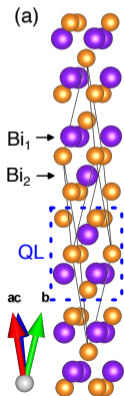
Henk *et al.*, PRL **109**, 076801 (2012)

Project "ML-Exc"

Magnetic co-doping of topological insulators

Bi_2Te_3

Dimer clusters of 3d, 4d transition metal defects

1-1:1 (R=4.38 Ang.) 1-2:0 (R=4.79 Ang.) 1-2:1 (R=6.10 Ang.) 1-2:2 (R=6.49 Ang.)

1-1:5 (R=11.35 Ang.) 1-1:6 (R=11.60 Ang.) 1-2:9 (R=11.76 Ang.) 1-1:7 (R=12.17 Ang.)

Single-impurity dabase, N=2'000.
go.fzj.de/judit

Dimer database, N=2'000[a].
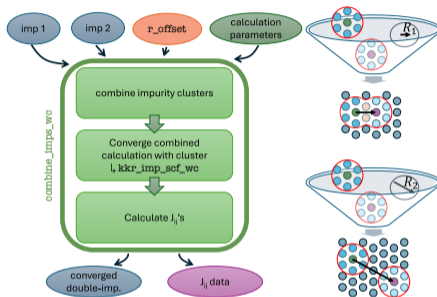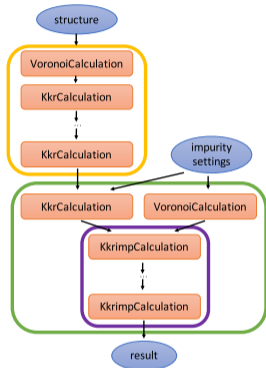
Co-doping can help to control

- critical T_c of QAHE
- exchange splitting Δ_{xc}
- long-range magnetic ordering

for applications in spintronics and fault-tolerant quantum computing.

[a]Mozumder et al. 2024.

Project "ML-Exc"

AiiDA-KKR workflows[2]

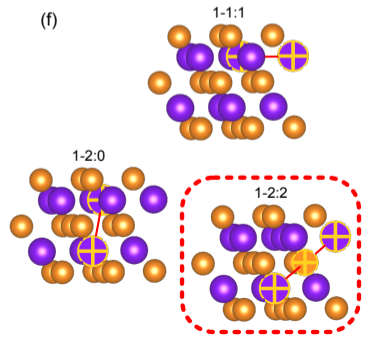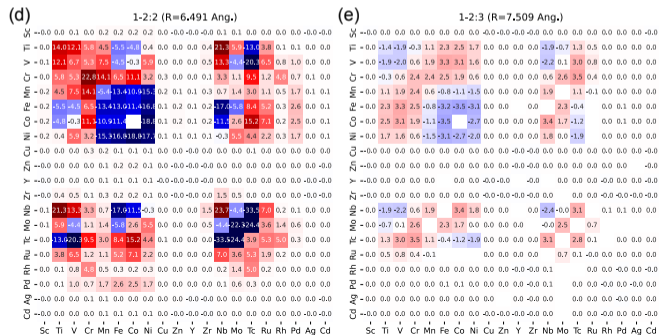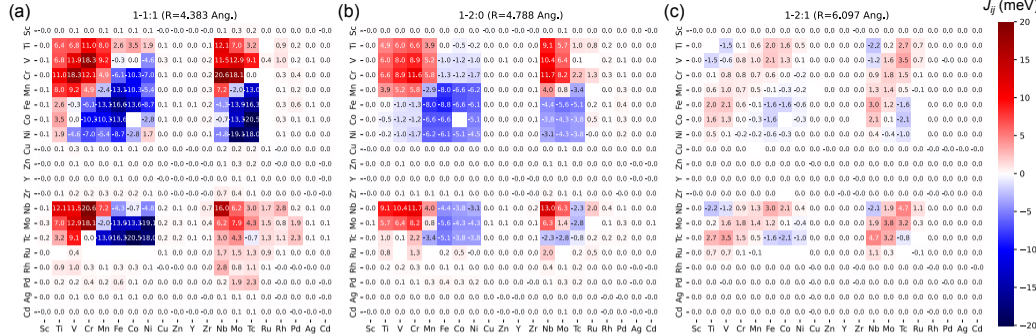Extended Heisenberg Hamiltonian. $H = -\frac{1}{2}\sum_{i,j} J_{ij}\, \vec{S}_i \cdot \vec{S}_j - \frac{1}{2}\sum_{i,j} \vec{D}_{ij} \cdot \left(\vec{S}_i \times \vec{S}_j\right)$
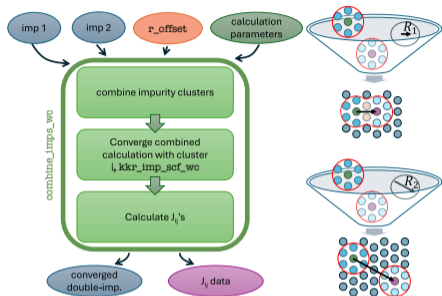
Exchange constants from method of infinitesimal rotations[1]. $\mathcal{J}_{ij} = -\frac{1}{\pi}\, \text{Im} \int_{-\infty}^{E_F} \mathrm{d}E\, \text{Tr}[\delta t_i G_{ij}\delta t_j G_{ji}]$

---

[1] Liechtenstein et al. 1987.
[2] Rüßmann, Bertoldo, and Blügel 2021.
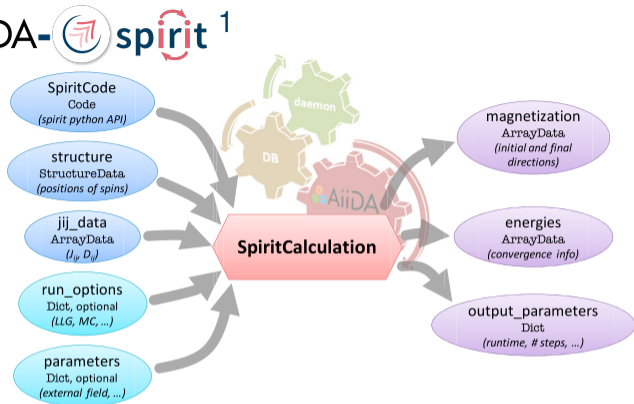
Spin dynamics with AiiDA-spirit [1]

Liechtenstein formula

$$\mathcal{J}_{ij} = -\frac{1}{\pi} \operatorname{Im} \int_{-\infty}^{E_F} \mathrm{d}E \operatorname{Tr}[\delta t_i G_{ij} \delta t_j G_{ji}]$$

ML-IAP approach.

$$E_k = \sum_k E_k \longrightarrow J_{ij} = \sum_k (J_{ij})_k$$

Landau-Lifshitz-Gilbert equation

$$\frac{\partial \vec{S}_i}{\partial t} = -\gamma' \vec{S}_i \times \vec{B}_i^{\mathrm{eff}} - \lambda \vec{S}_i \times \left(\vec{S}_i \times \vec{B}_i^{\mathrm{eff}} \right)$$

juspin.de

[1] Rüßmann, Ribas Sobreviela, et al. 2022.

Project "ML-Exc"
Model selection

Model	Citation	Type	CSSP	NN	Defects	Spin	Symmetry
AutoML	Conrad et al. 2022	Composition	X			-	-
Coulomb matrix	Rupp et al. 2012	Descriptor				-	explicit
SOAP	Bartók, Kondor, and Csányi 2013	Descriptor				-	explicit
Alchemical SOAP	Lopanitsyna et al. 2023	Potential	X			-	explicit
Disordered SOAP	Sommer et al. 2023	Descriptor			X	-	explicit
GAP	Bartók, Payne, et al. 2010	Potential	X			?	explicit
ACE	Bochkarev et al. 2022	Potential				-	explicit
MEGNetSparse	Kazeev et al. 2023	Potential	X	X	X	-	explicit
MACE	Batatia, Kovács, et al. 2022	Potential	X	X		-	explicit
MACE-MP	Batatia, Benner, et al. 2023	UIP	X	X		-	explicit
Magnetic ACE	Rinaldi et al. 2024	Potential				noco	explicit
SpinGNN++	Yu et al. 2024	Potential	X	X		noco	explicit
CHGNet	Deng et al. 2023	UIP	X	X		coll	explicit
SNRep	M. Domina, Cobelli, and Sanvito 2022	Potential				coll	explicit
PET	Pozdnyakov and Ceriotti 2024	Potential	?	X		coll	approximate

Project "ML-Exc"

Tensorial interaction

Heisenberg Hamiltonian in tensor form.

$$\mathcal{H}_H = -\sum_{j>i} \vec{m}_i \cdot \mathcal{J}_{ij} \vec{m}_j$$

Tensor components: isotropic, anti-symmetric (DMI) and anisotropic or traceless symmetric part (neglected so far).

$$\mathcal{J}_{ij} = J_{ij}\mathbb{1} + \mathcal{J}_{ij}^A + \mathcal{J}_{ij}^S$$

with $J_{ij}^{xx} = J_{ij}^{yy} = J_{ij}^{zz} = \frac{1}{3}J_{ij}$ and

$$\mathcal{J}_{ij}^A = \begin{bmatrix} 0 & J_{ij}^{xy} & J_{ij}^{xz} \\ J_{ij}^{yx} & 0 & J_{ij}^{yz} \\ J_{ij}^{zx} & J_{ij}^{zy} & 0 \end{bmatrix} = \begin{bmatrix} 0 & J_{ij}^{xy} & -J_{ij}^{zx} \\ -J_{ij}^{xy} & 0 & J_{ij}^{yz} \\ J_{ij}^{zx} & -J_{ij}^{yz} & 0 \end{bmatrix} = \begin{bmatrix} 0 & -D_{ij}^{z} & D_{ij}^{y} \\ D_{ij}^{z} & 0 & -D_{ij}^{x} \\ -D_{ij}^{y} & D_{ij}^{x} & 0 \end{bmatrix}$$

HIGHER-ORDER SPIN INTERACTION

✅ $H_1 = \sum_{ij}{}' J_{ij} \hat{\boldsymbol{S}}_i \cdot \hat{\boldsymbol{S}}_j$ (The bilinear term)

W. Heisenberg, Z. Physik **49**, 619 (1928): P. W. Anderson, Phys. Rev. **79**, 350 (1950)

✅ $H_2 = \sum_{ij}{}' B_{ij} \left(\hat{\boldsymbol{S}}_i \cdot \hat{\boldsymbol{S}}_j \right)^2$ (The biquadratic term)

P. W. Anderson, in *Magnetism* Vol. 1 (Academic Press, 1963): C. Kittel, Phys. Rev. **120**, 335 (1960).

✅ $H_3 = \sum_{ijkl}{}' K_{ijkl} \left[\left(\hat{\boldsymbol{S}}_i \cdot \hat{\boldsymbol{S}}_j \right) \left(\hat{\boldsymbol{S}}_k \cdot \hat{\boldsymbol{S}}_l \right) + \left(\hat{\boldsymbol{S}}_i \cdot \hat{\boldsymbol{S}}_l \right) \left(\hat{\boldsymbol{S}}_j \cdot \hat{\boldsymbol{S}}_k \right) - \left(\hat{\boldsymbol{S}}_i \cdot \hat{\boldsymbol{S}}_k \right) \left(\hat{\boldsymbol{S}}_j \cdot \hat{\boldsymbol{S}}_l \right) \right]$ (The ring exchange interaction term)

D. J. Thouless, Proc. Phys. Soc. **86**, 893 (1965)
M. Takahashi, J. Phys. C: Solid State Phys. **10**, 1298 (1977).

✅ $H_4 = \sum_{ijk}{}' Y_{ijk} \left(\hat{\boldsymbol{S}}_i \cdot \hat{\boldsymbol{S}}_j \right) \left(\hat{\boldsymbol{S}}_j \cdot \hat{\boldsymbol{S}}_k \right)$ (The 4-spin—3-site interaction term)

M. Hoffmann *et al.*, Phys. Rev. B **101**, 024418 (2020).

✅ $H^{CC} = -\frac{1}{2} \left[\hat{\boldsymbol{S}}_i \cdot \left(\hat{\boldsymbol{S}}_j \times \hat{\boldsymbol{S}}_k \right) \right] \tau_{ijk}^{\dagger} \kappa_{ii'}^{CC} \tau_{i'j'k'} \left[\hat{\boldsymbol{S}}_{i'} \cdot \left(\hat{\boldsymbol{S}}_{j'} \times \hat{\boldsymbol{S}}_{k'} \right) \right]$ (The chiral-chiral interaction term)

S. Grytsiuk *et al.*, Nat. Commun. **11**, 511 (2020).

✅ $\sum_{i,j,k}{}' \left(\hat{\boldsymbol{S}}_i \cdot \hat{\boldsymbol{S}}_j \right) \left(\hat{\boldsymbol{S}}_j \cdot \hat{\boldsymbol{S}}_k \right) \left(\hat{\boldsymbol{S}}_k \cdot \hat{\boldsymbol{S}}_i \right)$ (6-spin—3-site interaction term)

JÜLICH Forschungszentrum

RELATIVISTIC EXCHANGE INTERACTION

$$\hat{\mathcal{H}}_{\text{soc}} = -\lambda \sum_i \sum_m \sum_\mu \frac{\langle g_i(\boldsymbol{r})|\hat{L}_i^\mu|m_i(\boldsymbol{r})\rangle}{E_{i,m} - E_{i,g}} \left[\hat{S}_i^\mu, \ \hat{\mathcal{H}}^{(s)}\right]$$

Spin Hamiltonian

$J_{12}\hat{\boldsymbol{S}}_1 \cdot \hat{\boldsymbol{S}}_2 \longrightarrow \boldsymbol{D}_{12}^{\text{bl}} \cdot (\hat{\boldsymbol{S}}_1 \times \hat{\boldsymbol{S}}_2)$

$B_{12}(\hat{\boldsymbol{S}}_1 \cdot \hat{\boldsymbol{S}}_2)^2 \longrightarrow \boldsymbol{D}_{12}^{\text{bq}} \cdot \left[(\hat{\boldsymbol{S}}_1 \cdot \hat{\boldsymbol{S}}_2)(\hat{\boldsymbol{S}}_1 \times \hat{\boldsymbol{S}}_2) + (\hat{\boldsymbol{S}}_1 \times \hat{\boldsymbol{S}}_2)(\hat{\boldsymbol{S}}_1 \cdot \hat{\boldsymbol{S}}_2)\right]$

$K_{1234}\left[(\hat{\boldsymbol{S}}_1 \cdot \hat{\boldsymbol{S}}_2)(\hat{\boldsymbol{S}}_3 \cdot \hat{\boldsymbol{S}}_4)\right.$
$\left. +(\hat{\boldsymbol{S}}_1 \cdot \hat{\boldsymbol{S}}_4)(\hat{\boldsymbol{S}}_2 \cdot \hat{\boldsymbol{S}}_3) - (\hat{\boldsymbol{S}}_1 \cdot \hat{\boldsymbol{S}}_3)(\hat{\boldsymbol{S}}_2 \cdot \hat{\boldsymbol{S}}_4)\right]$
$\longrightarrow$

$\boldsymbol{D}_{12}^{\text{ring}} \cdot (\hat{\boldsymbol{S}}_3 \cdot \hat{\boldsymbol{S}}_4)(\hat{\boldsymbol{S}}_1 \times \hat{\boldsymbol{S}}_2) + \boldsymbol{D}_{34}^{\text{ring}} \cdot (\hat{\boldsymbol{S}}_1 \cdot \hat{\boldsymbol{S}}_2)(\hat{\boldsymbol{S}}_3 \times \hat{\boldsymbol{S}}_4)$
$+ \boldsymbol{D}_{14}^{\text{ring}} \cdot (\hat{\boldsymbol{S}}_2 \cdot \hat{\boldsymbol{S}}_3)(\hat{\boldsymbol{S}}_1 \times \hat{\boldsymbol{S}}_4) + \boldsymbol{D}_{23}^{\text{ring}} \cdot (\hat{\boldsymbol{S}}_1 \cdot \hat{\boldsymbol{S}}_4)(\hat{\boldsymbol{S}}_2 \times \hat{\boldsymbol{S}}_3)$
$- \left[\boldsymbol{D}_{13}^{\text{ring}} \cdot (\hat{\boldsymbol{S}}_2 \cdot \hat{\boldsymbol{S}}_4)(\hat{\boldsymbol{S}}_1 \times \hat{\boldsymbol{S}}_3) + \boldsymbol{D}_{24}^{\text{ring}} \cdot (\hat{\boldsymbol{S}}_1 \cdot \hat{\boldsymbol{S}}_3)(\hat{\boldsymbol{S}}_2 \times \hat{\boldsymbol{S}}_4)\right]$

$Y_{123} {\sum_{i,j,k}}' (\hat{\boldsymbol{S}}_i \cdot \hat{\boldsymbol{S}}_j)(\hat{\boldsymbol{S}}_j \cdot \hat{\boldsymbol{S}}_k)$

$$\sum_{i=1}^3 \boldsymbol{D}_\Delta^{\text{4-3}} \cdot \left[\hat{\boldsymbol{S}}_i \hat{\chi}_{123} + \hat{\chi}_{123}\hat{\boldsymbol{S}}_i - 2|\hat{\boldsymbol{S}}_1|^2(\hat{\boldsymbol{S}}_2 \times \hat{\boldsymbol{S}}_3) - 2|\hat{\boldsymbol{S}}_2|^2(\hat{\boldsymbol{S}}_3 \times \hat{\boldsymbol{S}}_1) - 2|\hat{\boldsymbol{S}}_3|^2(\hat{\boldsymbol{S}}_1 \times \hat{\boldsymbol{S}}_2)\right]$$

Community resources

Best of atomistic machine learning

Largest list of atomistic ML tools on the web (400+), auto-ranked, regular updates[a]

go.fzj.de/baml

---
[a]Wasmer et al. 2023.

Contents

Discussion slides

Solution in *k*- space for periodic systems

$$G_{LL'}^{nn'}(E) = g_{LL'}^{nn'}(E) + \sum_{n'',L''} g_{LL''}^{nn''}(E)\, t_{l''}^{n''}(E)\, G_{L''L'}^{n''n'}(E)$$

⇓   Fourier transformation of *G, g*

$$G_{LL'}(\vec{k}; E) = g_{LL'}(\vec{k}; E) + \sum_{L''} g_{LL''}(\vec{k}; E)\, t_{l''}(E)\, G_{L''L'}(\vec{k}; E) \longleftarrow$$

⇓   Matrix inversion

$$[G] = [g] + [g] \cdot [t] \cdot [G]$$

$$\boxed{G_{LL'}(\vec{k}; E) = \left[\left(1 - \boldsymbol{g}(\vec{k}; E)\, \boldsymbol{t}(E) \right)^{-1} \boldsymbol{g}(\vec{k}; E) \right]_{LL'}}$$

⇓   On-site term for charge density

$$G_{LL'}^{nn}(E) = \frac{1}{V_{\text{BZ}}} \int_{\text{BZ}} d^3k\, G_{LL'}(\vec{k}; E)$$

Framework:
One-electron states in a crystal

Self-consistent field $V(x)$; density-functional theory
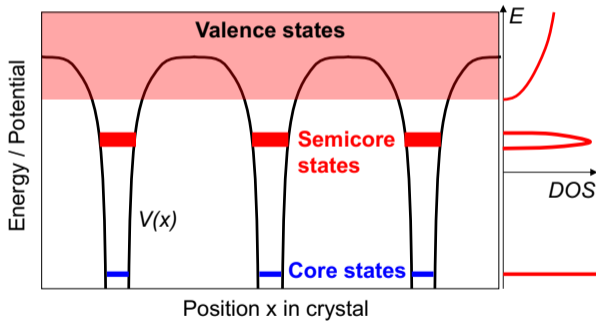
Complex energy contour

$$\rho_n(\vec{r}) = -\frac{2}{\pi}\text{Im}\int_{E_b}^{E_F} dE\, G(\vec{r}+\vec{R}^n, \vec{r}+\vec{R}^n; E)$$

Integration:
a lot of E-points

$$G(E) = \sum_{n\vec{k}} \frac{|\psi_{n\vec{k}}\rangle\langle\psi_{n\vec{k}}|}{E - \epsilon_{n\vec{k}}} \quad \text{Poles} \quad \longrightarrow \quad n(E) = \sum_{n\vec{k}} \delta(E - \epsilon_{n\vec{k}})$$

$$G(E+i\varepsilon) = \sum_{n\vec{k}} \frac{|\psi_{n\vec{k}}\rangle\langle\psi_{n\vec{k}}|}{E + i\varepsilon - \epsilon_{n\vec{k}}} \quad \longrightarrow \quad n(E+i\varepsilon) = \sum_{n\vec{k}} \frac{\varepsilon}{\varepsilon^2 + (E - \epsilon_{n\vec{k}})^2}$$

$\text{Im}E_1 < \text{Im}E_2 < \text{Im}E_3$
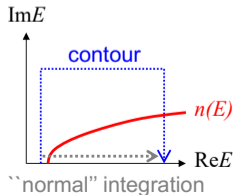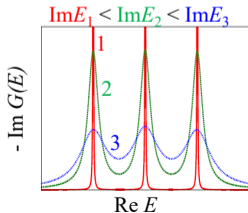
Lorenzian broadening
→ Less E-points for integration

$G(E)$ is analytical
→ Integral is the same.

``normal'' integration

Secular equation

Tessellation of space in atomic cells

Local solution of Schrödinger's equation in each cell
(spherical wave representation)

$$R_l(\vec{r}; E)\, Y_L(\hat{r})$$

In a sense: "optimal basis functions"

General solution:

$$\Psi_{\vec{k}}(\vec{r}) = \sum_L c_L(\vec{k}; E)\, R_l(\vec{r}; E)\, Y_L(\hat{r})$$

Insert into Schrödinger's eq. to obtain coefficients c_L

$$\sum_{L'} \left[\delta_{LL'} - t_l(E) g_{LL'}(\vec{k}; E) \right] c_{L'}(\vec{k}; E) = 0$$

Fourier-transformed coefficients of free-space Green function
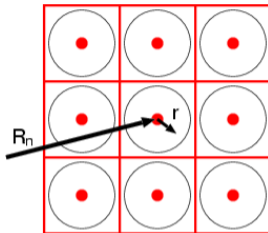
Multiple scattering

Bookkeeping:

1. $(\text{Incoming wave})_A = \displaystyle\sum_{n \in \{B, C, \dots\}} (\text{Outgoing waves})_n$

2. $\psi_{\vec{k}}^{\text{sc}\,(n)}(\vec{r}) = \displaystyle\sum_L b_{\vec{k}L}^{\text{sc}\,(n)} \, h_L(\vec{r}; E)$

   $\psi_{\vec{k}}^{\text{inc}\,(n')}(\vec{r}') = \displaystyle\sum_L b_{\vec{k}L}^{(n')} \, j_L(\vec{r}'; E)$

   related by *t*-matrix
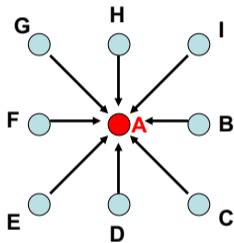
3. Transformation of Hankel functions:

$$h_L(\vec{r}' + \vec{R}^{n'} - \vec{R}^n; E) = \frac{i}{\sqrt{E}} \sum_{L'} g_{LL'}^{nn'}(E) \, j_{L'}(\vec{r}'; E)$$

4. Periodic system → Bloch property → *k*-space

$$\sum_{L'} \left(\delta_{LL'} - g_{LL'}(\vec{k}; E) \, t_{l'}(E) \right) c_{\vec{k}L'}^{(n')} = 0 \qquad \Psi_{\vec{k}}(\vec{r}) = \sum_L c_{\vec{k}L} \, R_L(\vec{r}; E)$$

KKR secular equation → $E = E(\vec{k})$

Fermi surfaces, scattering off impurities

Lippmann-Schwinger equation

$$\Psi_{\vec{k}}^{\mathrm{imp}}(\vec{r}) = \Psi_{\vec{k}}(\vec{r}) + \int d^3r \, G_0(\vec{r}, \vec{r}'; E) \left[V^{\mathrm{imp}}(\vec{r}) - V^{\mathrm{cryst}}(\vec{r}) \right] \Psi_{\vec{k}}^{\mathrm{imp}}(\vec{r})$$

t-matrix (transition amplitude)

$$T_{\vec{k}\vec{k}'} = (\Psi_{\vec{k}}, V_{\mathrm{imp}} \Psi_{\vec{k}'}^{\mathrm{imp}})$$

Scattering rate

$$w_{\vec{k}\vec{k}'} = 2\pi |T_{\vec{k}\vec{k}'}|^2 \, \delta(E_{\vec{k}} - E_{\vec{k}'})$$

Crystal momentum   Spin

Zn imp.

| 71 | 73 | 76 | 78 |

| 22722 | 33188 | 48475 | 70803 |
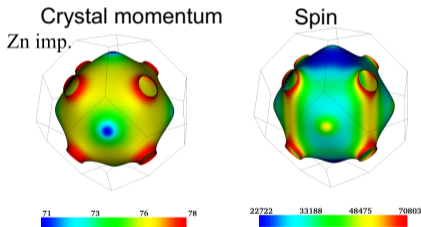
Finite lifetime (ps) of Fermi surf. states in fcc Cu due to scattering off 1% Zn impurities.

Summary

Green function method: Alternative to the Schrödinger equation

KKR Green function: Expansion in site-dependent scattering waves
with single-site and multiple-scattering part

$$G(\vec{r} + \vec{R}^n, \vec{r}' + \vec{R}^{n'}; E) =$$
$$-i\sqrt{E} \sum_L R_L^n(\vec{r}_<; E) H_L^n(\vec{r}_>; E) \delta_{nn'} + \sum_{LL'} R_L^n(\vec{r}; E) G_{LL'}^{nn'}(E) R_{L'}^{n'}(\vec{r}'; E)$$

Impurity problem: Dyson equation
Only perturbed sites need recalculation

$$G(E) = (E - H_0 - \Delta V)^{-1}$$
$$= [1 - G_0(E) \Delta V]^{-1} G_0(E)$$

Large systems > 10000 atoms: Sparse matrices allow for O(N) calculations
(*KKR-nano* method by R. Zeller et al.)

References I

📄 Bartók, Albert P., Risi Kondor, and Gábor Csányi (May 28, 2013). "On Representing Chemical Environments". In: Physical Review B 87.18, p. 184115. DOI: 10.1103/PhysRevB.87.184115. URL: https://link.aps.org/doi/10.1103/PhysRevB.87.184115.

📄 Bartók, Albert P., Mike C. Payne, et al. (Apr. 1, 2010). "Gaussian Approximation Potentials: The Accuracy of Quantum Mechanics, without the Electrons". In: Physical Review Letters 104.13, p. 136403. DOI: 10.1103/PhysRevLett.104.136403. URL: https://link.aps.org/doi/10.1103/PhysRevLett.104.136403.

📄 Batatia, Ilyes, Philipp Benner, et al. (Dec. 29, 2023). A Foundation Model for Atomistic Materials Chemistry. DOI: 10.48550/arXiv.2401.00096. arXiv: 2401.00096 [cond-mat, physics:physics]. URL: http://arxiv.org/abs/2401.00096. Pre-published.

📄 Batatia, Ilyes, Dávid Péter Kovács, et al. (June 15, 2022). MACE: Higher Order Equivariant Message Passing Neural Networks for Fast and Accurate Force Fields. DOI: 10.48550/arXiv.2206.07697. arXiv: 2206.07697 [cond-mat, physics:physics, stat]. URL: http://arxiv.org/abs/2206.07697v1. Pre-published.

References II

📄 Bochkarev, Anton et al. (Jan. 24, 2022). "Efficient Parametrization of the Atomic Cluster Expansion". In: Physical Review Materials 6.1, p. 013804. DOI: 10.1103/PhysRevMaterials.6.013804. URL: https://link.aps.org/doi/10.1103/PhysRevMaterials.6.013804.

📄 Bosoni, Emanuele et al. (Jan. 2024). "How to Verify the Precision of Density-Functional-Theory Implementations via Reproducible and Universal Workflows". In: Nature Reviews Physics 6.1, pp. 45–58. ISSN: 2522-5820. DOI: 10.1038/s42254-023-00655-3. URL: https://www.nature.com/articles/s42254-023-00655-3.

📄 Conrad, Felix et al. (Nov. 11, 2022). "Benchmarking AutoML for Regression Tasks on Small Tabular Data in Materials Design". In: Scientific Reports 12.1, p. 19350. ISSN: 2045-2322. DOI: 10.1038/s41598-022-23327-1. URL: https://www.nature.com/articles/s41598-022-23327-1.

References III

📄 Deng, Bowen et al. (Sept. 2023). "CHGNet as a Pretrained Universal Neural Network Potential for Charge-Informed Atomistic Modelling". In: Nature Machine Intelligence 5.9 (9), pp. 1031–1041. ISSN: 2522-5839. DOI: 10.1038/s42256-023-00716-3. URL: https://www.nature.com/articles/s42256-023-00716-3.

📄 Domina, M., M. Cobelli, and S. Sanvito (June 30, 2022). "Spectral Neighbor Representation for Vector Fields: Machine Learning Potentials Including Spin". In: Physical Review B 105.21, p. 214439. DOI: 10.1103/PhysRevB.105.214439. URL: https://link.aps.org/doi/10.1103/PhysRevB.105.214439.

📄 Domina, Michelangelo (Mar. 7, 2024). "The Jacobi-Legendre Framework for Machine Learning in Materials Investigation and Discovery". PhD thesis. Dublin: Trinity College Dublin. 184 pp. URL: http://hdl.handle.net/2262/106636.

References IV

Kazeev, Nikita et al. (June 26, 2023). "Sparse Representation for Machine Learning the Properties of Defects in 2D Materials". In: npj Computational Materials 9.1 (1), pp. 1–10. ISSN: 2057-3960. DOI: 10.1038/s41524-023-01062-z. URL: https://www.nature.com/articles/s41524-023-01062-z.

Liechtenstein, A. I. et al. (May 1, 1987). "Local Spin Density Functional Approach to the Theory of Exchange Interactions in Ferromagnetic Metals and Alloys". In: Journal of Magnetism and Magnetic Materials 67.1, pp. 65–74. ISSN: 0304-8853. DOI: 10.1016/0304-8853(87)90721-9. URL: https://www.sciencedirect.com/science/article/pii/0304885387907219.

Lopanitsyna, Nataliya et al. (Apr. 26, 2023). "Modeling High-Entropy Transition Metal Alloys with Alchemical Compression". In: Physical Review Materials 7.4, p. 045802. DOI: 10.1103/PhysRevMaterials.7.045802. URL: https://link.aps.org/doi/10.1103/PhysRevMaterials.7.045802.

References V

Mozumder, Rubel et al. (July 5, 2024). High-Throughput Magnetic Co-Doping and Design of Exchange Interactions in a Topological Insulator. arXiv: 2407.04413 [cond-mat]. URL: http://arxiv.org/abs/2407.04413. Pre-published.

Pozdnyakov, Sergey N. and Michele Ceriotti (Feb. 6, 2024). Smooth, Exact Rotational Symmetrization for Deep Learning on Point Clouds. DOI: 10.48550/arXiv.2305.19302. arXiv: 2305.19302 [cond-mat, physics:physics]. URL: http://arxiv.org/abs/2305.19302. Pre-published.

Rinaldi, Matteo et al. (Jan. 11, 2024). "Non-Collinear Magnetic Atomic Cluster Expansion for Iron". In: npj Computational Materials 10.1, pp. 1–12. ISSN: 2057-3960. DOI: 10.1038/s41524-024-01196-8. URL: https://www.nature.com/articles/s41524-024-01196-8.

References VI

Rupp, Matthias et al. (Jan. 31, 2012). "Fast and Accurate Modeling of Molecular Atomization Energies with Machine Learning". In: Physical Review Letters 108.5, p. 058301. DOI: 10.1103/PhysRevLett.108.058301. URL: https://link.aps.org/doi/10.1103/PhysRevLett.108.058301.

Rüßmann, Philipp, Fabian Bertoldo, and Stefan Blügel (Jan. 26, 2021). "The AiiDA-KKR Plugin and Its Application to High-Throughput Impurity Embedding into a Topological Insulator". In: npj Computational Materials 7.1 (1), pp. 1–9. ISSN: 2057-3960. DOI: 10.1038/s41524-020-00482-5. URL: https://www.nature.com/articles/s41524-020-00482-5.

Rüßmann, Philipp, Jordi Ribas Sobreviela, et al. (2022). "The AiiDA-Spirit Plugin for Automated Spin-Dynamics Simulations and Multi-Scale Modeling Based on First-Principles Calculations". In: Frontiers in Materials 9. ISSN: 2296-8016. DOI: 10.3389/fmats.2022.825043. URL: https://www.frontiersin.org/articles/10.3389/fmats.2022.825043.

References VII

Sommer, Timo et al. (Nov. 21, 2023). "3DSC - a Dataset of Superconductors Including Crystal Structures". In: Scientific Data 10.1 (1), p. 816. ISSN: 2052-4463. DOI: 10.1038/s41597-023-02721-y. URL: https://www.nature.com/articles/s41597-023-02721-y.

Wasmer, Johannes et al. (2023). Best of Atomistic Machine Learning. FZJ-2023-05862. Quanten-Theorie der Materialien. DOI: 10.5281/ZENODO.10430261. URL: https://juser.fz-juelich.de/record/1020061.

Yu, Hongyu et al. (Jan. 8, 2024). General Time-Reversal Equivariant Neural Network Potential for Magnetic Materials. DOI: 10.48550/arXiv.2211.11403. arXiv: 2211.11403 [cond-mat, physics:physics]. URL: http://arxiv.org/abs/2211.11403. Pre-published.